Cosmic QCD transition for large lepton flavor asymmetries

Mandy M. Middeldorf-Wygas,[1,*] Isabel M. Oldengott,[2,†] Dietrich Bödeker,[1,‡] and Dominik J. Schwarz[1,§]

[1]*Fakultät für Physik, Universität Bielefeld, Postfach 100131, 33501 Bielefeld, Germany*

[2]*Departament de Fisica Teòrica and IFIC, CSIC-Universitat de València, 46100 Burjassot, Spain*

(Received 19 October 2021; accepted 21 June 2022; published 28 June 2022)

We study the impact of large lepton flavor asymmetries on the cosmic QCD transition. Scenarios of *unequal* lepton flavor asymmetries are observationally almost unconstrained and therefore open up a whole new parameter space for the cosmic QCD transition. We find that for large asymmetries, the formation of a Bose-Einstein condensate of pions can occur and identify the corresponding parameter space. In the vicinity of the QCD transition scale, we express the pressure in terms of a Taylor expansion with respect to the complete set of chemical potentials. The Taylor coefficients rely on input from lattice QCD calculations from the literature. The domain of applicability of this method is discussed.

DOI: 10.1103/PhysRevD.105.123533

I. INTRODUCTION

The recent direct detection of gravitational waves (GWs) by the LIGO/Virgo Collaboration [1] has revived the interest in phase transitions in the early Universe [2]. In general, first-order phase transitions can be accompanied by processes that lead to the emission of GWs, while crossovers do not lead to a strong enhancement over the primordial GW spectrum. Within the Standard Model of particle physics (SM) at vanishing chemical potentials, both the electroweak transition at $T_{\rm ew} \sim 160$ GeV as well as the transition of quantum chromodynamics (QCD) at $T_{\rm QCD} \sim 150$ MeV are expected to be crossovers. However, many extensions of the scalar sector of the Standard Model can give rise to a first-order elelectroweak phase transition [3]. Even the simplest extension—i.e., by a real singlet—is difficult to exclude at the LHC (see, e.g., Ref. [4]). There are, however, much fewer mechanisms known that could provide a first-order QCD transition (e.g., Refs. [5–7]), which is why this possibility has obtained considerably less attention. The softening of the equation of state during the QCD transition, be it first order or a crossover, leads to an enhancement of the production of primordial black holes [8–10], one of the prime candidates for dark matter—see, e.g., Ref. [11].

Our current understanding of the QCD phase diagram is as follows: Whether strongly interacting particles exist in the form of quarks and gluons or in the form of hadrons (i.e., confined quarks and gluons) depends in general on the temperature T and the baryon chemical potential $\mu_{\rm B}$ (and all other potentials associated with relevant conserved quantum numbers) of the system. It is known from lattice QCD [12–14] that at vanishing chemical potentials the transition between these two phases is a crossover, where a pseudocritical temperature is calculated to be $T_{\rm QCD} = 156.5 \pm 1.5$ MeV by Ref. [15] and $T_{\rm QCD} = 158.0 \pm 0.6$ MeV by Ref. [16]. At large baryon chemical potential μ_B and vanishing temperatures, in contrast, effective models of QCD (like the Nambu–Jona-Lasinio model) predict a first-order chiral transition [17]. This leads to the speculation that there exists a critical line in the (μ_B, T) diagram which separates the two phases by a first-order transition and which is supposed to end in a second-order critical end point. Functional QCD methods predict this critical end point (CEP) to be located around $(\mu_B^{\rm CEP}, T^{\rm CEP}) = (672, 93)$ MeV [18].

The standard trajectory of the Universe in the QCD diagram is based on the assumption of tiny matter-antimatter asymmetries and is expected to start at large temperatures and low chemical potentials. Due to the expansion of space, the temperature decreases, and the baryon chemical potential is expected to remain small roughly until pion annihilation at $T \approx m_\pi/3$, when μ_B starts to approach the nucleon mass. Therefore, as mentioned above, the transition is expected to be a crossover. This idea of the standard cosmic trajectory is based on the observation that the Universe has an extremely small and well-measured baryon asymmetry,

$$b \equiv n_B/s = (8.70 \pm 0.06) \times 10^{-11}, \tag{1}$$

*m.wygas@physik.uni-bielefeld.de
†isabel.oldengott@uv.es
‡bodeker@physik.uni-bielefeld.de
§dschwarz@physik.uni-bielefeld.de

Published by the American Physical Society under the terms of the Creative Commons Attribution 4.0 International license. Further distribution of this work must maintain attribution to the author(s) and the published article's title, journal citation, and DOI. Funded by SCOAP³.

as inferred from Ref. [19]. Here n_B is the baryon density—i.e., the number of baryons minus the number of antibaryons per volume—and s is the entropy density. Furthermore, it is reasonable to assume an electric-charge-neutral Universe—i.e., a vanishing electric charge asymmetry, $q \equiv n_Q/s = 0$ [20]. If the lepton flavor asymmetries $l_\alpha = n_{L_\alpha}/s$ are of the same order of magnitude as b, this indeed implies a small baryon chemical potential μ_B at $T \gtrsim m_\pi/3$ [21,22]. However, observational constraints on the lepton asymmetry are much weaker (see, e.g., Ref. [23]), allowing in principle a lepton asymmetry that is many orders of magnitude larger than the baryon asymmetry. The impact of lepton flavor asymmetries on the abundance of weakly interacting dark matter has been studied in Ref. [24].

As shown in Refs. [21,22], for increasing values of the lepton asymmetry the cosmic trajectory is shifted towards larger values of μ_B. References [21,22] assumed the lepton flavor asymmetries l_α to have the same values (i.e., $l_\alpha = l/3$, where l is the total asymmetry).

In this work, we drop the assumption of equal lepton flavor asymmetries that we made in Ref. [22]. We show that scenarios of unequal lepton flavor asymmetries are even less constrained and therefore can have an even larger impact on the cosmic trajectory. It turns out that the chemical potentials can become so big that they may affect the nature of the cosmic QCD transition.

This article is organized as follows: In Sec. II, we summarize our method to calculate the cosmic trajectory. Section III discusses the situation of unequal lepton flavor asymmetries. Our main results are presented in Sec. IV, where we also discuss the limitations of our current method. Further details are provided in two appendixes. We conclude in Sec. V. All expressions of this work are provided in natural units—i.e., $c = \hbar = k_B = 1$.

II. METHOD

In this section, we summarize the method of Ref. [22] and also reveal an improvement to it in the high-temperature regime. For more details, we refer the reader to Refs. [21,22,25].

We assume that baryon number, lepton flavor, and electric charge, as well as the entropy, are conserved in a comoving volume between temperatures well above the QCD transition [26]—i.e., $T \sim 500$ MeV—and the onset of neutrino oscillations at $T \sim 10$ MeV. Each conserved charge $C \in \{B, Q, L_\alpha\}$ can be assigned a chemical potential μ_C. Then, from the pressure $p(T, \mu)$ computed in a grand canonical ensemble

$$\exp(pV/T) = \mathrm{tr}\,\exp\left[\left(\sum_C \mu_C C - H\right)/T\right], \tag{2}$$

one can obtain the charge densities through

$$n_C = \frac{\partial p}{\partial \mu_C}. \tag{3}$$

For an ideal gas, this gives

$$n_C = \sum_i C_i n_i(T, \mu_i), \tag{4}$$

where the sum runs over the contributing individual particle species with net number densities n_i and charges C_i. The chemical potentials of the individual particle species μ_i can be expressed through the chemical potential of the conserved charges μ_C—see, e.g., Refs. [21,27]:

$$\mu_i = \sum_C C_i \mu_C. \tag{5}$$

Depending on the temperature range, we express the charge asymmetries through either Eq. (3) or Eq. (4).

The basic idea of this work and Refs. [21,22] can be summarized as follows: The cosmic trajectory in the QCD phase diagram is determined by the conservation of l_α, b, and q—i.e., by the requirement that these quantities remain constant throughout the evolution of the Universe in the temperature range under consideration. The baryon asymmetry can be fixed to its observed value (see above) and we assume an electric-charge-neutral Universe, $q = 0$ [20]. This leaves us with the three lepton flavor asymmetries l_α as free input parameters.

In the presence of lepton flavor asymmetries, the μ_{L_α} values are nonzero. With nonvanishing μ_{L_α}, the electric charge in the lepton sector is nonvanishing. It has to be compensated by an electric charge in the quark sector. To obtain total electric charge equal to zero and baryon asymmetry (almost) zero, a nonzero μ_Q and μ_B are required. This implies that lepton flavor asymmetries may have an impact on the nature of the cosmic QCD transition if they are sufficiently large.

By numerically solving the conservation laws for 10 MeV $< T <$ 500 MeV for a given set of l_α, we obtain the Universe's trajectory in six-dimensional $(\mu_B, \mu_Q, \mu_{L_\alpha}, T)$ space. To account for the confinement of quarks into hadrons at $T_{\mathrm{QCD}} \sim 150$ MeV, we divide this temperature range into three different regimes that we will describe in the following. Leptons, on the other hand, can be treated at all times as an ideal gas: We calculate their thermodynamic quantities, such as the number densities on the rhs of Eq. (4), assuming Fermi-Dirac distributions. In the temperature regime of interest, it is entirely sufficient to treat neutrinos as massless particles.

A. Quark-gluon plasma (QGP, $T \gtrsim T_{\mathrm{QCD}}$)

In Ref. [22], we treated quarks and gluons as an ideal gas. Due to considerably strong gluonic interactions, this is, however, not a very good approximation. As we show in

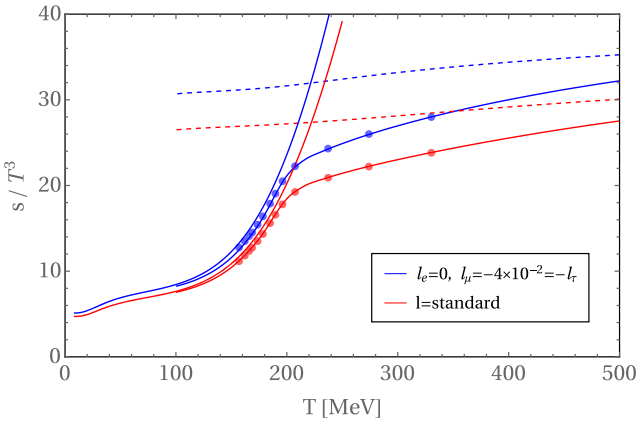

FIG. 1. Temperature evolution of the entropy density for the standard lepton asymmetry $l = -\frac{51}{28}b$ where $l_\alpha = \frac{l}{3}$, and for the case of unequilibrated lepton flavor asymmetries with $l_e = 0$, $l_\mu = -4 \times 10^{-2} = -l_\tau$. Continuous lines at low temperatures are results for the hadron residence gas. The symbols filled circles indicate results obtained using $2+1+1$ flavor lattice-QCD susceptibilities (Refs. [29,30]). The dashed lines are the ideal quark gas results. Continuous lines for high temperatures are the results using $\epsilon(T,0)$, and $p(T,0)$ including strong interaction effects according to Refs. [28,31] and the additional contributions for nonzero chemical potentials in the ideal gas approximation.

Fig. 1 for the entropy density, the ideal gas curves significantly deviate from the lattice results. In this work, we therefore use perturbative QCD corrections from Ref. [28] to the entropy density $s(T,0)$, the energy density $\epsilon(T,0)$, and the pressure $p(T,0)$. The calculations in Ref. [28] were performed at zero chemical potential. To account for nonzero chemical potentials, we add $s_{\rm id}(T,\mu) - s_{\rm id}(T,0)$, where $s_{\rm id}(T,\mu)$ is the ideal gas entropy. While these extra contributions are negligible for small lepton (flavor) asymmetries, they become sizeable for $|l_\alpha| \gtrsim 0.01$, as is apparent from Fig. 1. The charge asymmetries are calculated in the ideal gas limit as in Ref. [22]. In Appendix A, we show the impact on the cosmic trajectory of adding perturbative QCD corrections to the ideal quark gas result.

B. QCD phase (QCD, $T \approx T_{\rm QCD}$)

At temperatures around $T \sim 150$ MeV, quarks confine into hadrons and perturbative QCD can no longer be applied. As in Ref. [22], we therefore make use of susceptibilities χ_{ab} from lattice QCD to obtain a Taylor expansion of the QCD pressure:

$$p^{\rm QCD}(T,\mu) = p^{\rm QCD}(T,0) + \frac{1}{2}\mu_a\chi_{ab}(T)\mu_b + \mathcal{O}(\mu^4) \equiv p_0^{\rm QCD}(T) + p_2^{\rm QCD}(T,\mu), \quad (6)$$

with an implicit sum over $a,b \in \{B,Q\}$. Baryon and electric charge densities can then be expressed in terms of the chemical potentials through Eq. (3).

In [22], we presented results using two different datasets for the lattice QCD susceptibilities: (i) continuum extrapolated, including u, d, and s quarks [32], and (ii) not continuum-extrapolated but including also the c quark [29,30]. We showed that the inclusion of the charm quark is essential for connecting the different temperature regimes, which is why we only use the second dataset in this work. For the entropy density, we use the results for zero chemical potential from Ref. [28], which interpolate between HRG and perturbative QCD [31], and we add the nonzero μ contribution as in Eq. (6) [22]. Note that the entropy density obtained from the Taylor series almost perfectly agrees with the ideal quark gas result in Fig. 1 also at large chemical potentials. As we will see in Sec. IV, the use of lattice susceptibilities is nevertheless essential in order to connect the cosmic trajectory between the different temperature regimes.

C. Hadron resonance gas (HRG, $T \lesssim T_{\rm QCD}$)

As in Ref. [22], at low temperatures, we assume an ideal gas of hadron resonances (i.e., thermal distributions), taking into account hadron resonances up to mass $m_{\Lambda(2350)} \approx 2350$ MeV $\sim 15 T_{\rm QCD}$ according to the summary tables in Ref. [33].

III. LARGE LEPTON FLAVOR ASYMMETRIES

The baryon asymmetry of the Universe is a tiny and well-measured quantity. The origin of this number, however, cannot be explained within the SM of particle physics and gives rise to an active field of research. The idea of leptogenesis [34] is to create an initial lepton asymmetry that is partially converted into the baryon asymmetry by electroweak sphaleron processes. Therefore, according to the standard picture, the lepton asymmetry of our Universe would be on the same order of magnitude as the baryon asymmetry (i.e., tiny), or more explicitly $l = -\frac{51}{28}b$ [35], where the exact numerical prefactor depends on the assumed particle content of the Universe before the onset of sphaleron processes. This idea however still awaits experimental evidence and there are alternative models predicting large lepton asymmetries [36–41]. Either way, lepton asymmetry is a key parameter to understand the origin of the matter-antimatter asymmetry of the Universe.

When abandoning the assumption of a negligible lepton asymmetry, we are left with three lepton flavor asymmetries as free input parameters. In principle, those lepton flavor asymmetries can be initially different in size. At $T \approx 10$ MeV, neutrino oscillations become efficient, which can lead to an equilibration of lepton flavor asymmetries such that finally $l_\alpha \approx l/3$ [42,43]. It should be noted that depending on the initial values of the lepton flavor asymmetries and the mixing angles, equilibration may be only partial—i.e., $l_\alpha \neq l/3$ [44–46]. However, assuming that $l_\alpha = l/3$ after the onset of neutrino oscillations allows

us to obtain constraints on l from the observation of primordial elements—i.e., big bang nucleosynthesis (BBN) [47] and the cosmic microwave background (CMB) [23]. In Ref. [22], for simplicity we assumed equal lepton flavor asymmetries, $l_\alpha = l/3$. By numerically solving the conservation laws as explained in the previous section, we showed that for increasing values of $|l|$, the trajectory passes through larger absolute values of the chemical potentials μ_i ($i = B, Q, L_\alpha$). For the maximally allowed value $|l| < 1.2 \times 10^{-2}$ from CMB observations [23], the lattice susceptibilities allowed us to connect the QGP and HRG phases relatively smoothly (given the expected uncertainties from our approximations and the lattice QCD results). This result, however, was based on the assumption of equal lepton flavor asymmetries, and in this work we investigate the by far less constrained scenario of unequal lepton flavor asymmetries. In that case, since the total lepton asymmetry is conserved during neutrino oscillations, we are still constrained by $|l| < 1.2 \times 10^{-2}$ [23], but the magnitudes of the individual lepton flavor asymmetries could be much larger than $|l|$ as long as they fulfill $|l_e + l_\mu + l_\tau| < 1.2 \times 10^{-2}$. It was shown in Ref. [48] that such scenarios also lead to values of the effective number of relativistic degrees of freedom N_{eff} that are in agreement with BBN and CMB observations—i.e., $N_{\text{eff}} \sim 3$.

IV. COSMIC TRAJECTORY

The fact that the individual lepton flavor asymmetries are essentially unconstrained before the onset of neutrino oscillations opens up a huge parameter space for the cosmic trajectory at the time of the QCD transition. This raises the question of whether large enough lepton flavor asymmetries could change the nature of the QCD transition. Before exploring this new parameter space in Sec. IV C, we demonstrate that our current method does not allow us to study arbitrary large lepton flavor asymmetries.

Despite the observational constraint $|l| = |l_e + l_\mu + l_\tau| < 1.2 \times 10^{-2}$, unequal flavor asymmetries provide a lot of parameter freedom. For simplicity, in the main part of this work we only present the results for the scenario $l_e = 0$, $l_\mu = -l_\tau$. We refer the reader to Appendix B for more examples of differently distributed lepton flavor asymmetries. As a supplement to our previous work [22], we also discuss the case of equal flavor asymmetries.

A. Pion condensation

Within the HRG approximation, a large chemical potential of the electric charge μ_Q can lead to the formation of a Bose-Einstein condensate of pions. This happens when the chemical potential of the pion becomes larger than its mass—i.e., $|\mu_Q| = \mu_\pi \geq m_\pi$. While this in general could have interesting consequences such as the formation of pion stars [49,50], our computation does not apply, because we have not included a condensate.

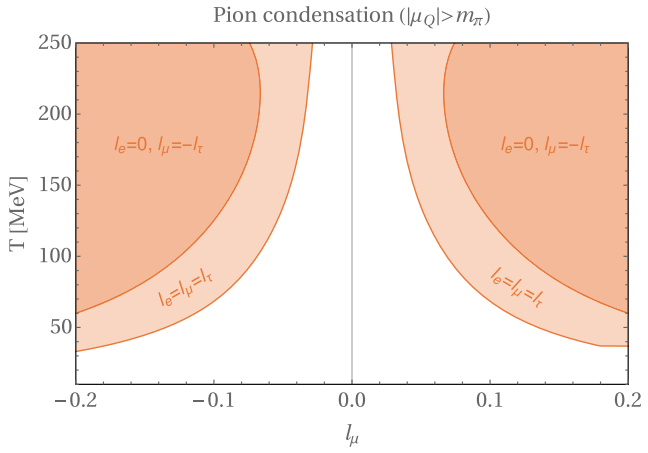

FIG. 2. Values of the muon lepton asymmetry l_μ for which pion condensation ($|\mu_Q| > m_\pi$) can occur, depending on the temperature. Dark shaded regions are for the case of unequal lepton flavor asymmetries with $l_e = 0$, $l_\mu = -l_\tau$; light shaded regions are for equal lepton flavor asymmetries $l_e = l_\mu = l_\tau = \frac{l}{3}$.

The condition $|\mu_Q| \geq m_\pi$ (and $q = 0$) translates nontrivially into the $(\mu_B, \mu_{L_e}, \mu_{L_\mu}, \mu_{L_\tau})$-$T$ planes. In order to determine the region of parameter space $(\mu_B, \mu_{L_e}, \mu_{L_\mu}, \mu_{L_\tau})$ in which pion condensation could happen, we add $|\mu_Q| = m_\pi$ as an additional condition on top of the conservation laws. While in general the three values for l_α are free to choose as input parameters, this extra condition fixes one degree of freedom, and therefore only two lepton flavor asymmetries can be chosen freely, while the third one is determined at each temperature T by numerically solving the conservation laws *and* $|\mu_Q| = m_\pi$.

Figure 2 shows the solutions of this set of equations for two different parameter choices: equal lepton flavor asymmetries ($l_e = l_\mu = l_\tau = \frac{l}{3}$) and unequal lepton flavor asymmetries exemplary for $l_e = 0$, $l_\mu = -l_\tau$. Note that both of these cases are effectively described by only one degree of freedom, and therefore no further input is required. The shaded regions in Fig. 2 show for which value of the muon lepton asymmetry l_μ pion condensation may occur at a given temperature. Figure 2 is consistent with the findings of Ref. [51], which includes a complementary study of the conditions for a pion condensate. Since the lepton flavor asymmetries are conserved quantities (before the onset of neutrino oscillations), we should choose the most conservative value for l_μ from Fig. 2 in order to avoid the appearance of pion condensation. As is evident from Fig. 2, for unequal lepton flavor asymmetries this constrains the reliability of our method to $|l_\mu| \lesssim 0.06$, and for equal flavor asymmetries to $|l_\mu| \lesssim 0.03$ (i.e., $|l| \lesssim 0.09$).

B. Applicability of Taylor expansion

Another restriction for our results comes from the truncation of the Taylor expansion (6) at second order. It

is naturally expected to break down at large chemical potentials, which restricts the applicability of our computation to sufficiently low values of the lepton asymmetries. There is, however, no strict criterion which tells us when exactly the use of Eq. (6) is still justified. A reasonable and conservative estimate could be given by

$$p_2^{\mathrm{QCD}}(T,\mu) \leq 0.1 \cdot p_0^{\mathrm{QCD}}(T)$$
$$\Rightarrow \frac{1}{2}\mu_a \chi_{ab} \mu_b \leq 0.1 \cdot p_0^{\mathrm{QCD}}(T). \quad (7)$$

As for the identification of the potential pion condensation region, we extend our numerical code by adding Eq. (7) as a sixth condition in addition to the conservation laws. Again, this reduces the number of degrees of freedom by 1, such that only two of the three lepton flavor asymmetries are free to choose.

Similarly to Fig. 2, we show the solution of this set of equations for the cases of equal lepton flavor asymmetries ($l_\alpha = \frac{l}{3}$) and unequal lepton flavor asymmetries (again, exemplary for $l_e = 0$, $l_\mu = -l_\tau$) in Fig. 3. It turns out that for the unequal case and for the largest temperature value of the lattice data, Eq. (7) is never fulfilled, such that the orange region in Fig. 3 ends below this temperature value. We conclude that the application of the Taylor expansion in Eq. (6) is justified for $|l_\mu| \lesssim 0.04$ in the case of unequal lepton flavor asymmetries, and for $|l_\mu| \lesssim 0.025$ (i.e., $|l| \lesssim 0.075$) in the case of equal flavor asymmetries. These constraints are hence slightly more restrictive than the ones from avoiding pion condensation.

C. Cosmic trajectory for large lepton flavor asymmetries

In Fig. 4, we show the cosmic trajectory projected on the (μ_B, T) and (μ_Q, T) planes for the case of unequal flavor asymmetries ($l_e = 0$, $l_\mu = -l_\tau$) and the case of equal flavor asymmetries ($l_\alpha = \frac{l}{3}$). We present both cases for their maximally allowed values for the lepton (flavor) asymmetries. As we have seen in the previous subsection, the unequal case is restricted by the applicability of the Taylor expansion to $|l_\mu| \lesssim 4 \times 10^{-2}$. For the equal case, our method is reliable for lepton asymmetries as large as $|l| = 7.5 \times 10^{-2}$, but observations of the CMB constrain the lepton asymmetry to $|l| < 1.2 \times 10^{-2}$ [23] (i.e., $|l_\alpha| < 4 \times 10^{-3}$). This also implies that all trajectories presented in our previous work [22] were affected neither by the restrictions from pion condensation nor by the applicability of the Taylor expansion. For comparison, we also show the standard trajectory (equal lepton flavor asymmetries with $l = -\frac{51}{28}b$). The shaded regions in Fig. 4 refer to the same regions as Figs. 2 and 3, but in the (μ_B, T) and (μ_Q, T) planes—i.e., the region where pion condensation occurs and the region where the second-order Taylor expansion is not reliable. It turns out that those

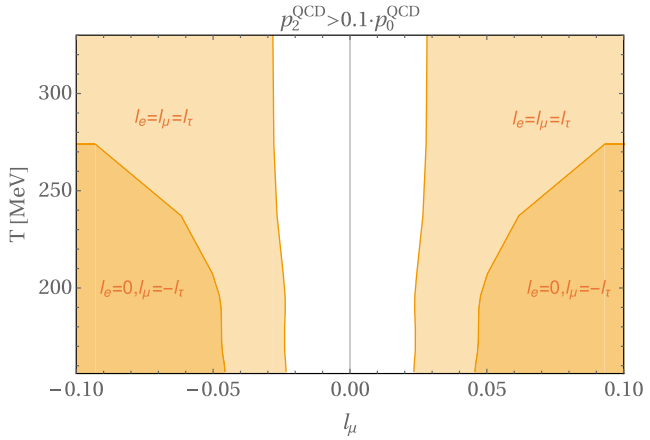

FIG. 3. Values of the muon lepton flavor asymmetry l_μ for which the use of the Taylor expansion becomes questionable $[p_2^{\mathrm{QCD}}(T,\mu) > 0.1 p_0^{\mathrm{QCD}}(T)]$, depending on the temperature. Light shaded regions are for the case of unequal lepton flavor asymmetries $l_e, l_\mu = -l_\tau$; dark shaded regions are for equal lepton flavor asymmetries $l_e = l_\mu = l_\tau = \frac{l}{3}$.

shaded regions are valid for both cases (equal and unequal lepton flavor asymmetries).

We see that both cases lead to trajectories reaching sizeable values of μ_B and μ_Q. Figure 4 furthermore confirms that at the QCD epoch, unequal lepton flavor asymmetries can induce larger chemical potentials than equal flavor asymmetries, because the latter case is constrained by CMB observations. However, Fig. 4 indicates that at high temperatures, the case of equal lepton flavor asymmetries leads to increasing values of $|\mu_B|$ and $|\mu_Q|$, whereas the trajectories of unequal lepton flavor asymmetries seem to bend toward small values of $|\mu_B|$ and $|\mu_Q|$. This is confirmed by Fig. 5, which shows the same cosmic trajectories as Fig. 4, but for temperatures in the GeV range. In the ultrarelativistic limit, the trajectories are indeed only a function of b and the total lepton asymmetry l, which is equal to zero for the blue curves. This can be shown by a straightforward generalization of the analytical estimates of μ_B and μ_Q in Sec. 2.1 of Ref. [21].

As is particularly apparent from the μ_Q plot in Fig. 4, for lepton asymmetries as large as those studied in this work, there is also a relatively large gap between the results for the QGP and the QCD phases, and as well between the HRG and the QCD phases. We believe that possible reasons for this could be related to the lack of continuum extrapolation and the restricted temperature range of lattice susceptibilities. Another impact could be given by missing finite density effects in the perturbative QCD calculations applied in this work [28]. Furthermore, as stated in Sec. IV B, there is no strict criterion for estimating the maximal lepton flavor asymmetries for which the use of the Taylor expansion [Eq. (6)] is still justified. This also means that there is no guarantee that the criterion applied in this work, Eq. (7), is indeed sufficiently conservative.

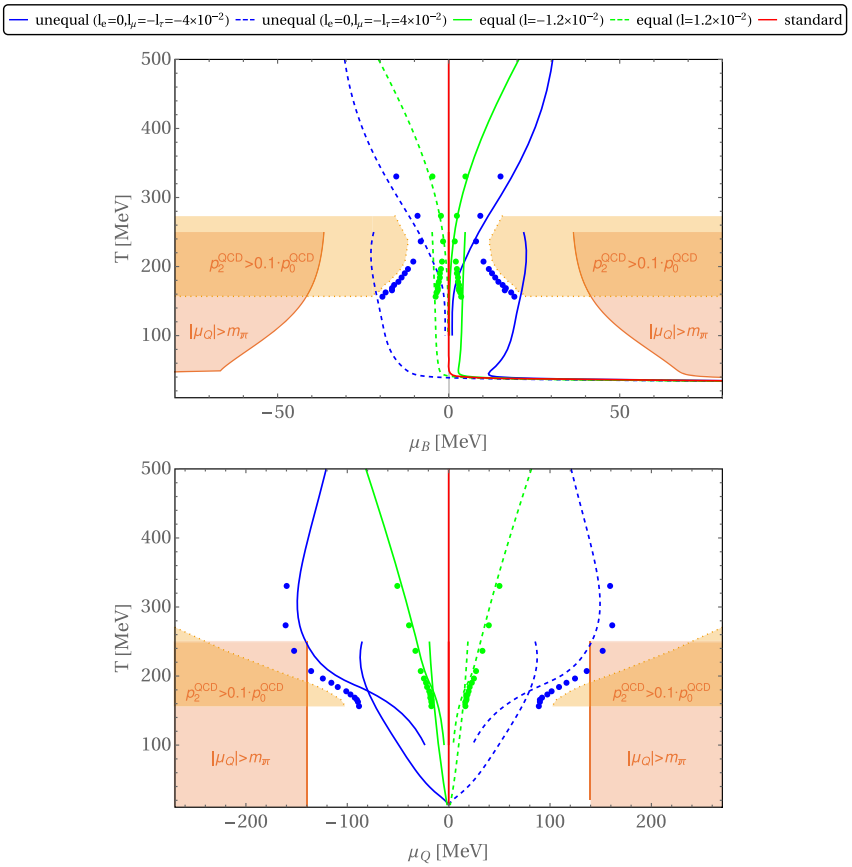

FIG. 4. Cosmic trajectories projected onto the (μ_B, T) plane (upper) and the (μ_Q, T) plane (lower) for different choices of the lepton flavor asymmetries l_α, calculated for the three temperature regimes described in Sec. II. Shaded regions refer to the regions where pion condensation may occur ($|\mu_Q| > m_\pi$) and where the applicability of the Taylor expansion becomes unreliable ($p_2^{\mathrm{QCD}} > 0.1 \cdot p_0^{\mathrm{QCD}}$), both discussed in Secs. IV A and IV B.

Note that for the scenario of $l_\mu = 0$, $l_e = -l_\tau$, the corresponding curves in Fig. 4 would look extremely similar to the case presented here. The scenario of $l_\tau = 0$, $l_e = -l_\mu$, in contrast, is restricted to much smaller values of μ_B and μ_Q.

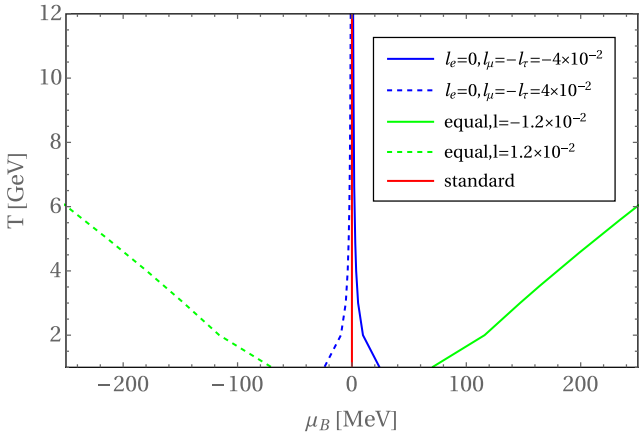

FIG. 5. Same as upper plot of Fig. 4, but at higher temperatures.

V. CONCLUSIONS

We extended our previous work [22] and studied the cosmic trajectory in the QCD phase diagram for large *unequal lepton flavor asymmetries*. We argued that scenarios of unequal flavor asymmetries are much less constrained than the previously studied case of equal lepton flavor asymmetries: While for equal lepton flavor asymmetries CMB constraints [23] restrict the magnitudes of the individual lepton flavor asymmetries to relatively small values, in the case of unequal lepton flavor asymmetries they are essentially unconstrained (as long as their sum fulfills the CMB requirement $|l_e + l_\mu + l_\tau| < 1.2 \times 10^{-2}$ [23]). Exemplary for the scenario of $l_e = 0$, $l_\mu = -l_\tau$ we showed that the cosmic trajectory indeed reaches larger μ_B and μ_Q than are reachable for equal flavor asymmetries. This extends the parameter space to the region of the QCD diagram in which the nature of the QCD transition is still unknown. In fact, QCD studies until now do not give a conclusive answer about the existence of a CEP, and therefore, about the possibility of first-order transition. The lack of a full theoretical understanding of the QCD

phase diagram actually calls for a study of the phenomenological consequences of a first-order vs crossover transition at high lepton flavor asymmetries, which perhaps allows us to rule out one of the possibilities. At the same time, the impact of lepton asymmetries on the QCD epoch offers a very interesting perspective to gain insights to the origin of the matter-antimatter asymmetry of the Universe: If for large enough l_α the transition turns out to be first order, the prospect of measuring the GW spectrum with pulsar timing arrays [52] would offer a way to observationally constrain individual lepton flavor asymmetries (before the onset of neutrino oscillations).

However, we also showed that our current method is not capable to be applied to lepton flavor asymmetries which imply *significantly* larger values of μ_B and μ_Q than already studied in our previous work [22]. When the electric charge chemical potential exceeds the pion mass, a Bose-Einstein condensation of pions might form. For scenarios of both equal and unequal asymmetries, we determined under which conditions this may happen. While the possible formation of a pion condensate is a phenomenon that must be explored further [53], in practice for our method, it simply implies that our treatment of the low-momentum modes of pions is not sufficient any longer. This could be circumvented by including the possibility of a pion condensate into our method [54]. However, the more serious restriction to our method comes from the applicability of a Taylor expansion, in which we use lattice QCD susceptibilities. We showed that for $|l_\mu| \gtrsim 4 \times 10^{-2}$, the chemical potentials become as large as $p_2^{\mathrm{QCD}}(T,\mu) > 0.1 \cdot p_0^{\mathrm{QCD}}(T)$—i.e., the second-order contribution becomes a sizeable correction to the zeroth-order contribution, which makes the Taylor series approach questionable. This problem could be relaxed by the use of higher-order contributions to the QCD pressure; such are, however, currently not available from lattice QCD calculations including the charm quark. Alternatively to the application of lattice susceptibilities might be the application of functional QCD methods [55] which do not encounter any problems in the regime of large chemical potentials and predict the existence of a CEP at $(\mu_{u/d}^{\mathrm{CEP}}, T^{\mathrm{CEP}}) \approx (200, 110)$ MeV [18]. The access to the phase structure in the whole (μ, T) plane could offer a consistent platform to investigate the cosmic trajectory at QCD temperatures, even though the truncations introduced in functional QCD methods would bring in some ambiguities on determining the phase structure quantitatively.

Our final conclusion is that large lepton flavor asymmetries still allow for the possibility of a first-order cosmic QCD transition. Extending our study to sufficiently large lepton flavor asymmetries with the presently applied method described in Ref. [22], based on Taylor expansions around vanishing chemical potentials, is, however, not possible, and further improvements are required.

ACKNOWLEDGMENTS

We thank Fei Gao, Frithjof Karsch, Jürgen Schaffner-Bielich and Christian Schmidt for interesting discussions. We acknowledge support by the Deutsche Forschungsgemeinschaft (DFG) through Grant No. CRC-TR 211, "Strong-interaction matter under extreme conditions." M. M. M.-W. acknowledges the support by Studienstiftung des Deutschen Volkes. I. M. O. acknowledges support from FPA2017-845438 and the Generalitat Valenciana under Grant No. PROMETEOII/2017/033.

APPENDIX A: IMPACT OF PERTURBATIVE QCD CORRECTIONS IN THE HIGH-TEMPERATURE REGIME

As described in the main text of Sec. II, in this work we improved our method in the high-temperature regime upon our previous work [22]: While we described quarks

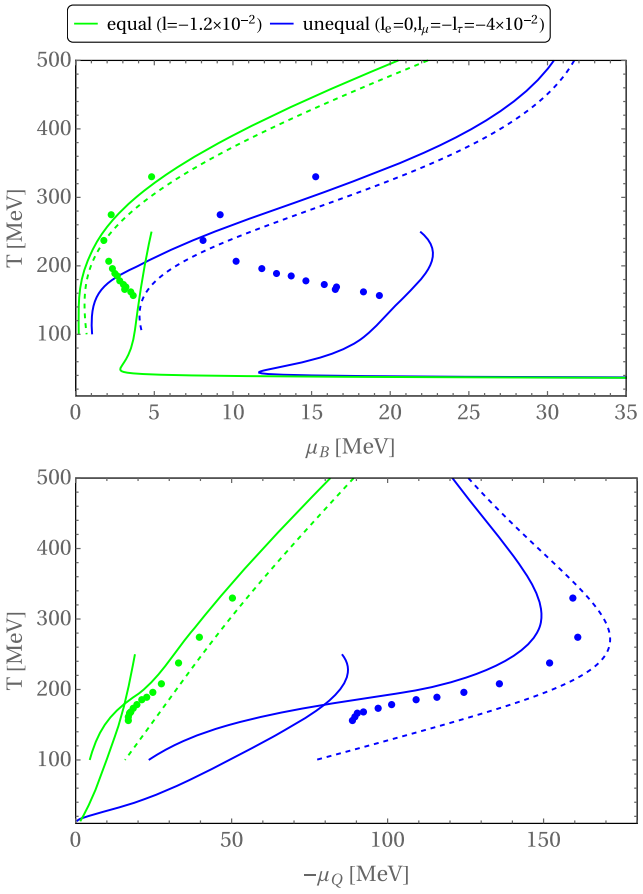

FIG. 6. Cosmic trajectories projected onto the (μ_B, T) plane (upper) and the (μ_Q, T) plane (lower) for different choices of the lepton flavor asymmetries l_α. Solid lines include corrections from perturbative QCD [28] (applied in this work); dashed lines assume an ideal gas of gluons and quarks (applied in Ref. [22]).

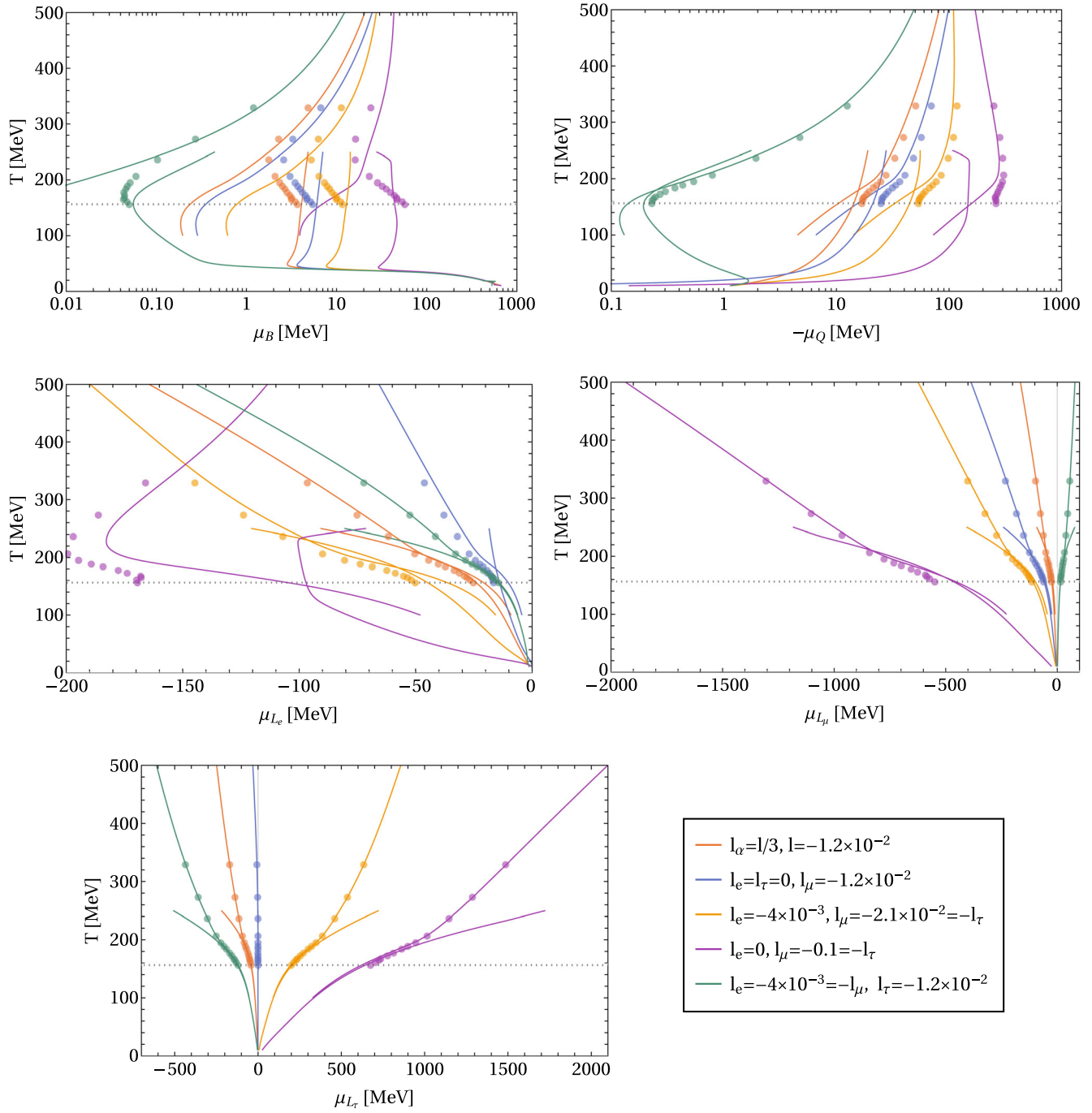

FIG. 7. Temperature evolution of conserved charge chemical potentials for different cases of unequal lepton flavor asymmetries. Top left: baryon chemical potential μ_B. Top right: electric charge chemical potential $-\mu_Q$. Middle left: electron lepton flavor chemical potential μ_{L_e}. Middle right: muon lepton flavor chemical potential μ_{L_μ}. Bottom left: tau lepton flavor chemical potential μ_{L_τ}. Notations as before.

and gluons at high temperatures as an ideal gas in Ref. [22], we here take into account corrections from perturbative QCD [28]. In this appendix, we show how the inclusion of these corrections impacts the cosmic trajectory. Figure 6 shows that the perturbative corrections (solid lines) significantly shift the cosmic trajectories compared to the ideal quark gas (dashed lines) applied in Ref. [22].

APPENDIX B: DIFFERENT CASES OF UNEQUAL LEPTON FLAVOR ASYMMETRIES

In this appendix, we show the cosmic trajectories for a variety of different choices of the lepton flavor asymmetries l_α in Fig. 7. Note that a common plot with the restrictions to our method, as in Fig. 4, is not feasible, since the different trajectories refer to different contours for pion condensation and the applicability of the Taylor expansion.

[1] B. P. Abbott *et al.* (LIGO Scientific, Virgo Collaborations), Observation of Gravitational Waves from a Binary Black Hole Merger, Phys. Rev. Lett. **116**, 061102 (2016).

[2] C. Caprini and D. G. Figueroa, Cosmological backgrounds of gravitational waves, Classical Quantum Gravity **35**, 163001 (2018).

[3] J. Espinosa and M. Quiros, The electroweak phase transition with a singlet, Phys. Lett. B **305**, 98 (1993).

[4] M. Cepeda *et al.*, Report from working group 2: Higgs physics at the HL-LHC and HE-LHC, CERN Yellow Rep. Monogr. **7**, 221 (2019).

[5] S. Iso, P. D. Serpico, and K. Shimada, QCD-Electroweak First-Order Phase Transition in a Supercooled Universe, Phys. Rev. Lett. **119**, 141301 (2017).

[6] D. Bödeker, Remarks on the QCD-electroweak phase transition in a supercooled universe, Phys. Rev. D **104**, L111501 (2021).

[7] T. Hambye, A. Strumia, and D. Teresi, Super-cool dark matter, J. High Energy Phys. 08 (2018) 188.

[8] K. Jedamzik, Primordial black hole formation during the QCD epoch, Phys. Rev. D **55**, R5871 (1997).

[9] K. Jedamzik and J. C. Niemeyer, Primordial black hole formation during first order phase transitions, Phys. Rev. D **59**, 124014 (1999).

[10] C. T. Byrnes, M. Hindmarsh, S. Young, and M. R. S. Hawkins, Primordial black holes with an accurate QCD equation of state, J. Cosmol. Astropart. Phys. 08 (2018) 041.

[11] B. Carr and F. Kuhnel, Primordial black holes as dark matter: Recent developments, Annu. Rev. Nucl. Part. Sci. **70**, 355 (2020).

[12] Y. Aoki, G. Endrodi, Z. Fodor, S. D. Katz, and K. K. Szabo, The order of the quantum chromodynamics transition predicted by the standard model of particle physics, Nature (London) **443**, 675 (2006).

[13] T. Bhattacharya *et al.*, QCD Phase Transition with Chiral Quarks and Physical Quark Masses, Phys. Rev. Lett. **113**, 082001 (2014).

[14] H.-T. Ding, F. Karsch, and S. Mukherjee, Thermodynamics of strong-interaction matter from lattice QCD, Int. J. Mod. Phys. E **24**, 1530007 (2015).

[15] A. Bazavov *et al.* (HotQCD Collaboration), Chiral crossover in QCD at zero and non-zero chemical potentials, Phys. Lett. B **795**, 15 (2019).

[16] S. Borsanyi, Z. Fodor, J. N. Guenther, R. Kara, S. D. Katz, P. Parotto, A. Pasztor, C. Ratti, and K. K. Szabo, QCD Crossover at Finite Chemical Potential from Lattice Simulations, Phys. Rev. Lett. **125**, 052001 (2020).

[17] M. Asakawa and K. Yazaki, Chiral restoration at finite density and temperature, Nucl. Phys. **A504**, 668 (1989).

[18] F. Gao and J. M. Pawlowski, QCD phase structure from functional methods, Phys. Rev. D **102**, 034027 (2020).

[19] N. Aghanim *et al.* (Planck Collaboration), Planck 2018 results: VI. Cosmological parameters, Astron. Astrophys. **641**, A6 (2020); Erratum, Astron. Astrophys. **652**, C4 (2021).

[20] C. Caprini, S. Biller, and P. G. Ferreira, Constraints on the electrical charge asymmetry of the Universe, J. Cosmol. Astropart. Phys. 02 (2005) 006.

[21] D. J. Schwarz and M. Stuke, Lepton asymmetry and the cosmic QCD transition, J. Cosmol. Astropart. Phys. 11 (2009) 025; Erratum, J. Cosmol. Astropart. Phys. 10 (2010) 01.

[22] M. M. Wygas, I. M. Oldengott, D. Bödeker, and D. J. Schwarz, Cosmic QCD Epoch at Nonvanishing Lepton Asymmetry, Phys. Rev. Lett. **121**, 201302 (2018).

[23] I. M. Oldengott and D. J. Schwarz, Improved constraints on lepton asymmetry from the cosmic microwave background, Europhys. Lett. **119**, 29001 (2017).

[24] M. Stuke, D. J. Schwarz, and G. Starkman, WIMP abundance and lepton (flavour) asymmetry, J. Cosmol. Astropart. Phys. 03 (2012) 040.

[25] M. M. Wygas, Large lepton asymmetry and the cosmic QCD transition, Ph.D., University Bielefeld (main), 2019.

[26] In the Standard Model, baryon number and lepton flavor numbers are conserved below the electroweak sphaleron freeze-out temperature $T_{\rm sph} \simeq 131$ GeV.

[27] J. I. Kapusta and C. Gale, *Finite-Temperature Field Theory: Principles and Applications* (Cambridge University Press, Cambridge, England, 2011).

[28] M. Laine and M. Meyer, Standard Model thermodynamics across the electroweak crossover, J. Cosmol. Astropart. Phys. 07 (2015) 035.

[29] A. Bazavov *et al.*, The melting and abundance of open charm hadrons, Phys. Lett. B **737**, 210 (2014).

[30] S. Mukherjee, P. Petreczky, and S. Sharma, Charm degrees of freedom in the quark gluon plasma, Phys. Rev. D **93**, 014502 (2016).

[31] M. Laine and Y. Schroder, Quark mass thresholds in QCD thermodynamics, Phys. Rev. D **73**, 085009 (2006).

[32] A. Bazavov *et al.* (HotQCD Collaboration), Fluctuations and correlations of net baryon number, electric charge, and strangeness: A comparison of lattice QCD results with the hadron resonance gas model, Phys. Rev. D **86**, 034509 (2012).

[33] M. Tanabashi *et al.* (Particle Data Group), Review of particle physics, Phys. Rev. D **98**, 030001 (2018).

[34] M. Fukugita and T. Yanagida, Baryogenesis without grand unification, Phys. Lett. B **174**, 45 (1986).

[35] E. W. Kolb and M. S. Turner, Grand unified theories and the origin of the baryon asymmetry, Annu. Rev. Nucl. Part. Sci. **33**, 645 (1983).
[36] S. Eijima and M. Shaposhnikov, Fermion number violating effects in low scale leptogenesis, Phys. Lett. B **771**, 288 (2017).
[37] J. Ghiglieri and M. Laine, Precision study of GeV-scale resonant leptogenesis, J. High Energy Phys. 02 (2019) 014.
[38] J. A. Harvey and E. W. Kolb, Grand unified theories and the lepton number of the Universe, Phys. Rev. D **24**, 2090 (1981).
[39] I. Affleck and M. Dine, A new mechanism for baryogenesis, Nucl. Phys. **B249**, 361 (1985).
[40] L. Canetti, M. Drewes, T. Frossard, and M. Shaposhnikov, Dark matter, baryogenesis and neutrino oscillations from right handed neutrinos, Phys. Rev. D **87**, 093006 (2013).
[41] M. Drewes, Y. Georis, and J. Klarić, Mapping the Viable Parameter Space for Testable Leptogenesis, Phys. Rev. Lett. **128**, 051801 (2022).
[42] A. D. Dolgov, S. H. Hansen, S. Pastor, S. T. Petcov, G. G. Raffelt, and D. V. Semikoz, Cosmological bounds on neutrino degeneracy improved by flavor oscillations, Nucl. Phys. **B632**, 363 (2002).
[43] Y. Y. Y. Wong, Analytical treatment of neutrino asymmetry equilibration from flavor oscillations in the early Universe, Phys. Rev. D **66**, 025015 (2002).
[44] S. Pastor, T. Pinto, and G. G. Raffelt, Relic Density of Neutrinos with Primordial Asymmetries, Phys. Rev. Lett. **102**, 241302 (2009).
[45] G. Barenboim, W. H. Kinney, and W.-I. Park, Resurrection of large lepton number asymmetries from neutrino flavor oscillations, Phys. Rev. D **95**, 043506 (2017).
[46] L. Johns, M. Mina, V. Cirigliano, M. W. Paris, and G. M. Fuller, Neutrino flavor transformation in the lepton-asymmetric universe, Phys. Rev. D **94**, 083505 (2016).
[47] C. Pitrou, A. Coc, J.-P. Uzan, and E. Vangioni, Precision big bang nucleosynthesis with improved helium-4 predictions, Phys. Rep. **754**, 1 (2018).
[48] G. Mangano, G. Miele, S. Pastor, O. Pisanti, and S. Sarikas, Updated BBN bounds on the cosmological lepton asymmetry for non-zero θ_{13}, Phys. Lett. B **708**, 1 (2012).
[49] H. Abuki, T. Brauner, and H. J. Warringa, Pion condensation in a dense neutrino gas, Eur. Phys. J. C **64**, 123 (2009).
[50] B. B. Brandt, G. Endrodi, E. S. Fraga, M. Hippert, J. Schaffner-Bielich, and S. Schmalzbauer, New class of compact stars: Pion stars, Phys. Rev. D **98**, 094510 (2018).
[51] V. Vovchenko, B. B. Brandt, F. Cuteri, G. Endrődi, F. Hajkarim, and J. Schaffner-Bielich, Pion Condensation in the Early Universe at Nonvanishing Lepton Flavor Asymmetry and Its Gravitational Wave Signatures, Phys. Rev. Lett. **126**, 012701 (2021).
[52] C. Tiburzi, Pulsars probe the low-frequency gravitational sky: Pulsar Timing Arrays basics and recent results, Pub. Astron. Soc. Aust. **35**, e013 (2018).
[53] See Ref. [51] for a study of the signal in primordial gravitational waves from a pion condensate.
[54] B. B. Brandt, G. Endrodi, and S. Schmalzbauer, QCD phase diagram for nonzero isospin-asymmetry, Phys. Rev. D **97**, 054514 (2018).
[55] C. S. Fischer, QCD at finite temperature and chemical potential from Dyson-Schwinger equations, Prog. Part. Nucl. Phys. **105**, 1 (2019).